EDN: RSIPYX
УДК 538.945

Changes of the Fermi Surface Topology in the Three-orbital Model for Iron Pnictides with the Spin-orbit Coupling

Danil A. Ivanov*
Yuliya N. Togushova†
Siberian Federal University
Krasnoyarsk, Russian Federation
Maxim M. Korshunov‡
Kirensky Institute of Physics
Federal Research Center KSC SB RAS
Krasnoyarsk, Russian Federation
Siberian Federal University
Krasnoyarsk, Russian Federation

Received 11.08.2023, received in revised form 21.09.2023, accepted 30.10.2023

Abstract. Effect of the spin-orbit coupling on the band structure and the Fermi surface of the three-orbital model is studied. The inter-orbital part of the model is reformulated to fully conform with the iron lattice symmetry. Because there are two iron ions in the unit cell, we introduce the intra- and inter-ion spin-orbit coupling constants to separate the effect of the related couplings on the band structure and the Fermi surface. Both the intra- and inter-ion parts lift the degeneracy of some bands at the $\Gamma = (0, 0)$ point and the splitting of bands along the $(0, \pi) - (\pi, \pi)$ direction of the Brillouin zone. We show that the inter-ion part of the spin-orbit coupling leads to the topological change of the Fermi surface — the splitting of two Fermi surface sheets around the $M = (\pi, \pi)$ point.

Keywords: Fe-based superconductors, spin-orbit coupling, band structure, Fermi surface.

Citation: D.A. Ivanov, Yu.N. Togushova, M.M. Korshunov, Changes of the Fermi Surface Topology in the Three-orbital Model for Iron Pnictides with the Spin-orbit Coupling, J. Sib. Fed. Univ. Math. Phys., 2023, 16(6), 795–803. EDN: RSIPYX.

Iron pnictides and chalcogenides represent systems with the intriguing mixture of different states including superconductivity, magnetism, nematic state, and some coexisting states [1–3]. The variety of exotic phases is naturally stems from the multiband nature of the systems [4]. From the density-functional theory (DFT) we know that the Fermi surface (FS) in iron-based systems is formed by several bands with the dominating contribution from the three t_{2g} iron d-orbitals. Hybridization of the xz, yz, and xy orbitals results in two electron-like Fermi surface sheets around $M = (\pi, \pi)$ point and two to three hole-like sheets around $\Gamma = (0, 0)$ point of the Brillouin zone (BZ) corresponding to the crystallographic unit cell that includes two iron ions. Such a Brillouin zone often called '2-Fe BZ' or 'folded BZ'. For the single-layer iron-pnictides the folding wave vector is two-dimensional and equals to $\mathbf{Q} = (\pi, \pi)$. DFT band structures and most of the experimental results are reported in the folded BZ since crystallographically it is

*danik.aliw@gmail.com
†ytogushova@sfu-kras.ru
‡mkor@iph.krasn.ru https://orcid.org/0000-0001-9355-2872

the correct one. Nesting between electron and hole sheets may produce the spin-density wave antiferromagnetic order in the undoped systems [5]. Destruction of the perfect nesting with the doping destroys long-range antiferromagnetic order, however, the scattering on the wave vector connecting hole and electron sheets remains strong. It is the most probable candidate for the interaction that drives superconducting pairing. Within the spin-fluctuation approach it results in the sign-changing extended s-wave gap ($s_\pm$ state) as the leading instability [4, 6–10].

There are several experimental findings pointing towards the non-vanishing role of the spin-orbit (SO) coupling. One of them is the anisotropy of the spin resonance peak violating the spin-rotational invariance, $\langle S_+ S_- \rangle = 2 \langle S_z S_z \rangle$, that have to be obeyed in the disordered system. It was observed in the inelastic neutron scattering [11]. Spin-rotational invariance violation within the three-orbital model was found to be due to the effect of the SO interaction [24] similar to the case of Sr_2RuO_4 [13]. Another intriguing fact comes from the superconducting gap studies via the multiple Andreev reflections [14, 15]. The expected number of distinct gaps in LiFeAs is two – one at the inner FS around the Γ-point, another one at the outer FS around the Γ-point and the same at the FS around the M-point. However, the analysis of the Andreev spectra reveals three different gaps [16, 17]. The observation may be explained by the FS topology change due to the SO interaction: the two crossing FS sheets around the M-point may become split into the inner and outer parts with the different gaps at each new part.

Several low-energy models with the minimal number of orbitals have been suggested for iron-based superconductors [18–23]. Here we focus on the three-orbital model from Ref. [23]. It is quite simple yet describes the most important bands coming from the t_{2g} manifold: the d_{xz} and d_{yz} orbitals are hybridized to form two electron Fermi surface sheets and one hole sheet around Γ point while the second one comes from the d_{xy} orbital. Within the model, the role of the SO coupling has been studied before [24], however, the model has a fundamental drawback — C_4 symmetry is broken for the large values of the SO coupling constant λ. Here we modify the model to avoid the violation of the symmetry and study the effect of the SO coupling on the topology of the Fermi surface and the band structure in the 2-Fe BZ.

1. Three-orbital model for the one-iron unit cell

Hamiltonian of the three-orbital model for the set of d-orbital of a *single* iron has the form [23]:

$$H_0^{(1)} = \sum_{\mathbf{k},\sigma,l,m} \varepsilon_{\mathbf{k}}^{lm} c_{\mathbf{k}l\sigma}^\dagger c_{\mathbf{k}m\sigma}, \tag{1}$$

where $c_{\mathbf{k}l\sigma}^\dagger$ ($c_{\mathbf{k}m\sigma}$) is the creation (annihilation) operator of a particle with momentum $\mathbf{k}$, spin σ, and orbital index l (m). We choose the following numbering of orbitals, $1 \to d_{xy}$, $2 \to d_{yz}$, $3 \to d_{zx}$. We introduce vector operators in the orbital space, $\hat{\Psi}_{\mathbf{k}\sigma}^\dagger = \left(c_{\mathbf{k}1\sigma}^\dagger, c_{\mathbf{k}2\sigma}^\dagger, c_{\mathbf{k}3\sigma}^\dagger \right)$, and rewrite the Hamiltonian as

$$H_0^{(1)} = \sum_{\mathbf{k},\sigma} \hat{\Psi}_{\mathbf{k}\sigma}^\dagger \hat{\varepsilon}_{\mathbf{k}} \hat{\Psi}_{\mathbf{k}\sigma}, \tag{2}$$

where the matrix of one-electron energies and hoppings has the form:

$$\hat{\varepsilon}_{\mathbf{k}} = \begin{pmatrix} \varepsilon_{1\mathbf{k}} & 0 & 0 \\ 0 & \varepsilon_{2\mathbf{k}} & \varepsilon_{4\mathbf{k}} \\ 0 & \varepsilon_{4\mathbf{k}} & \varepsilon_{3\mathbf{k}} \end{pmatrix}. \tag{3}$$

Here

$$\varepsilon_{1\mathbf{k}} = \epsilon_{xy} - \mu + 2t_{xy}(\cos k_x + \cos k_y) + 4t'_{xy}\cos k_x \cos k_y, \quad (4)$$

$$\varepsilon_{2\mathbf{k}} = \epsilon_{yz} - \mu + 2t_x \cos k_x + 2t_y \cos k_y + 4t' \cos k_x \cos k_y + 2t''(\cos 2k_x + \cos 2k_y), \quad (5)$$

$$\varepsilon_{3\mathbf{k}} = \epsilon_{xz} - \mu + 2t_y \cos k_x + 2t_x \cos k_y + 4t' \cos k_x \cos k_y + 2t''(\cos 2k_x + \cos 2k_y), \quad (6)$$

with μ being the chemical potential.

Previously, $\varepsilon_{4\mathbf{k}}$ was a function of $\sin k_x/2 \sin k_y/2$ [23,24]. Such a combination does not belong to the basis functions of the tetragonal group D_{4h}. It leads to the violation of the C_4 symmetry for the large SO coupling, i.e., $(0,0)-(\pi,0)$ and $(0,0)-(0,\pi)$ directions become inequivalent. The problem comes from the $k_{x,y}/2$ argument. To avoid it, we use the new expression for $\varepsilon_{4\mathbf{k}}$:

$$\varepsilon_{4\mathbf{k}} = 4t_{xzyz} \sin k_x \sin k_y + 3t''' \sin 2k_x \sin 2k_y. \quad (7)$$

We use the following set of parameters (in eV) that allows to reproduce the topology of the FS in iron-based systems: $\epsilon_{xy} = -0.70$, $\epsilon_{yz} = -0.34$, $\epsilon_{xz} = -0.34$, $t_{xy} = 0.18$, $t'_{xy} = 0.06$, $t_x = 0.26$, $t_y = -0.22$, $t' = 0.2$, $t'' = -0.07$, $t''' = 0.025$, $t_{xzyz} = 0.055$.

For the *single* iron, the spin-orbit coupling terms can be written as [25]

$$H_{SO}^{(1)} = \lambda \sum_f \mathbf{L}_f \cdot \mathbf{S}_f = \mathrm{i}\frac{\lambda}{2} \sum_{l,m,n} \epsilon_{lmn} \sum_{\mathbf{k},\sigma,\sigma'} c^\dagger_{\mathbf{k}l\sigma} c_{\mathbf{k}m\sigma'} \hat{\sigma}^n_{\sigma\sigma'}, \quad (8)$$

where λ is the SO coupling constant, $\mathbf{L}_f$ and $\mathbf{S}_f$ are the angular momentum and spin operators at the lattice site f, respectively, ϵ_{lmn} is the completely antisymmetric tensor, indices l, m, n take values $\{d_{yz}, d_{zx}, d_{xy}\}$, and $\hat{\sigma}^n_{\sigma\sigma'}$ are the Pauli spin matrices.

Explicit form of the Hamiltonian in terms of the vector operators is

$$H_{SO}^{(1)} = \sum_{\mathbf{k},\sigma,\sigma'} \hat{\Psi}^\dagger_{\mathbf{k}\sigma} \hat{\varepsilon}^{\sigma\sigma'}_{SO} \hat{\Psi}_{\mathbf{k}\sigma'}. \quad (9)$$

Here

$$\hat{\varepsilon}^{\sigma\sigma'}_{SO} = \mathrm{i}\frac{\lambda}{2} \begin{pmatrix} 0 & -\mathrm{i}\delta_{\sigma',\bar{\sigma}}\mathrm{sgn}\,(\sigma) & \delta_{\sigma',\bar{\sigma}} \\ \mathrm{i}\delta_{\sigma',\bar{\sigma}}\mathrm{sgn}\,(\sigma) & 0 & \delta_{\sigma',\sigma}\mathrm{sgn}\,(\sigma) \\ -\delta_{\sigma',\bar{\sigma}} & -\delta_{\sigma',\sigma}\mathrm{sgn}\,(\sigma) & 0 \end{pmatrix} = \quad (10)$$

$$= \mathrm{i}\frac{\lambda}{2} \left[\hat{\varepsilon}^z \delta_{\sigma',\sigma}\mathrm{sgn}\,(\sigma) + \delta_{\sigma',\bar{\sigma}} \left(\hat{\varepsilon}^x - \mathrm{i}\hat{\varepsilon}^y \mathrm{sgn}\,(\sigma)\right)\right], \quad (11)$$

where we have introduced the following matrices,

$$\hat{\varepsilon}^z = \begin{pmatrix} 0 & 0 & 0 \\ 0 & 0 & 1 \\ 0 & -1 & 0 \end{pmatrix} = \mathrm{i}J_x, \quad \hat{\varepsilon}^x = \begin{pmatrix} 0 & 0 & 1 \\ 0 & 0 & 0 \\ -1 & 0 & 0 \end{pmatrix} = -\mathrm{i}J_y, \quad \hat{\varepsilon}^y = \begin{pmatrix} 0 & 1 & 0 \\ -1 & 0 & 0 \\ 0 & 0 & 0 \end{pmatrix} = \mathrm{i}J_z. \quad (12)$$

Here, J_i are the generators of the rotation group $O(3)$.

The total Hamiltonian for the single iron, $H^{(1)} = H_0^{(1)} + H_{SO}^{(1)}$, can be written as

$$H^{(1)} = \sum_{\mathbf{k},\sigma} \left[\hat{\Psi}^\dagger_{\mathbf{k}\sigma} \left(\hat{\varepsilon}_{\mathbf{k}} + \mathrm{i}\frac{\lambda}{2}\hat{\varepsilon}^z \mathrm{sgn}\,(\sigma)\right) \hat{\Psi}_{\mathbf{k}\sigma} + \mathrm{i}\frac{\lambda}{2} \hat{\Psi}^\dagger_{\mathbf{k}\sigma} \left(\hat{\varepsilon}^x - \mathrm{i}\hat{\varepsilon}^y \mathrm{sgn}\,(\sigma)\right) \hat{\Psi}_{\mathbf{k}\bar{\sigma}}\right] =$$

$$= \sum_{\mathbf{k}} \begin{pmatrix} \hat{\Psi}^\dagger_{\mathbf{k}\uparrow} & \hat{\Psi}^\dagger_{\mathbf{k}\downarrow} \end{pmatrix} \cdot \hat{H}^{(1)} \cdot \begin{pmatrix} \hat{\Psi}_{\mathbf{k}\uparrow} \\ \hat{\Psi}_{\mathbf{k}\downarrow} \end{pmatrix}, \quad (13)$$

where

$$\hat{H}^{(1)} = \begin{pmatrix} \hat{\varepsilon}_{\mathbf{k}} + \mathrm{i}\frac{\lambda}{2}\hat{\varepsilon}^z & \mathrm{i}\frac{\lambda}{2}\hat{\varepsilon}^x + \frac{\lambda}{2}\hat{\varepsilon}^y \\ \mathrm{i}\frac{\lambda}{2}\hat{\varepsilon}^x - \frac{\lambda}{2}\hat{\varepsilon}^y & \hat{\varepsilon}_{\mathbf{k}} - \mathrm{i}\frac{\lambda}{2}\hat{\varepsilon}^z \end{pmatrix}. \tag{14}$$

Note that ε^x- and ε^y-components of the SO coupling mix spin-up and spin-down matrix elements thus effectively increasing the dimensionality of the problem by a factor of two.

2. Three-orbital model for the two-iron unit cell

To work in the crystallographic unit cell containing two irons, we make the folding procedure: momenta in Hamiltonian (1) are transformed as $(k_x + k_y)/2 \to k'_x$, $(k_x - k_y)/2 \to k'_y$ and the Hamiltonian matrix is doubled by adding the shifted $\varepsilon^{lm}_{\mathbf{k}'+\mathbf{Q}}$, where $\mathbf{Q} = (\pi, \pi)$ is the folding wave vector. For convenience, we skip prime assuming that all momenta are within the 2-Fe BZ and end up with the following Hamiltonian [24]

$$H_0 = \sum_{\mathbf{k},\sigma,l,m} \varepsilon^{lm}_{\mathbf{k}} c^\dagger_{\mathbf{k}l\sigma} c_{\mathbf{k}m\sigma} + \sum_{\mathbf{k},\sigma,l,m} \varepsilon^{lm}_{\mathbf{k}+\mathbf{Q}} c^\dagger_{\mathbf{k}+\mathbf{Q}l\sigma} c_{\mathbf{k}+\mathbf{Q}m\sigma}. \tag{15}$$

It can be written in the matrix form analogous to (13),

$$H = \sum_{\mathbf{k}} \begin{pmatrix} \hat{\Psi}^\dagger_{\mathbf{k}\uparrow} & \hat{\Psi}^\dagger_{\mathbf{k}\downarrow} & \hat{\Phi}^\dagger_{\mathbf{k}\uparrow} & \hat{\Phi}^\dagger_{\mathbf{k}\downarrow} \end{pmatrix} \cdot \hat{H} \cdot \begin{pmatrix} \hat{\Psi}_{\mathbf{k}\uparrow} \\ \hat{\Psi}_{\mathbf{k}\downarrow} \\ \hat{\Phi}_{\mathbf{k}\uparrow} \\ \hat{\Phi}_{\mathbf{k}\downarrow} \end{pmatrix}, \tag{16}$$

where $\hat{\Psi}_{\mathbf{k}\sigma}$ ($\hat{\Phi}_{\mathbf{k}\sigma}$) corresponds to the first (second) iron in the unit cell.

As for the SO coupling, we make the following conjecture [24]: the structure of the SO coupling between two orbitals on neighboring irons is the same as the structure between two orbitals on a single iron ion. As in Ref. [24], we assign different coupling constant to the intra-ion SO interaction (λ) and the inter-ion one (λ'). Note that the wording 'inter-ion SO coupling' does not necessary mean a long-range SO coupling like that in the Rashba effect. The SO interaction may be local, however, since orbitals of two neighboring irons hybridize directly and through As ion, the wave functions of electrons on those orbitals can overlap. It opens up a possibility for the effective inter-ion SO coupling.

For the intra-ion SO coupling, $\hat{H}$ has the form that immediately follows from (14):

$$\hat{H}^{\mathrm{intra}}_{SO} = \left(\begin{array}{cc|cc} \hat{\varepsilon}_{\mathbf{k}} + \mathrm{i}\frac{\lambda}{2}\hat{\varepsilon}^z & \mathrm{i}\frac{\lambda}{2}\hat{\varepsilon}^x + \frac{\lambda}{2}\hat{\varepsilon}^y & 0 & 0 \\ \mathrm{i}\frac{\lambda}{2}\hat{\varepsilon}^x - \frac{\lambda}{2}\hat{\varepsilon}^y & \hat{\varepsilon}_{\mathbf{k}} - \mathrm{i}\frac{\lambda}{2}\hat{\varepsilon}^z & 0 & 0 \\ \hline 0 & 0 & \hat{\varepsilon}_{\mathbf{k}+\mathbf{Q}} + \mathrm{i}\frac{\lambda}{2}\hat{\varepsilon}^z & \mathrm{i}\frac{\lambda}{2}\hat{\varepsilon}^x + \frac{\lambda}{2}\hat{\varepsilon}^y \\ 0 & 0 & \mathrm{i}\frac{\lambda}{2}\hat{\varepsilon}^x - \frac{\lambda}{2}\hat{\varepsilon}^y & \hat{\varepsilon}_{\mathbf{k}+\mathbf{Q}} - \mathrm{i}\frac{\lambda}{2}\hat{\varepsilon}^z \end{array}\right). \tag{17}$$

For the inter-ion SO coupling we have

$$\hat{H}^{\mathrm{inter}}_{SO} = \left(\begin{array}{cc|cc} 0 & 0 & \mathrm{i}\frac{\lambda'}{2}\hat{\varepsilon}^z & \mathrm{i}\frac{\lambda'}{2}\hat{\varepsilon}^x + \frac{\lambda'}{2}\hat{\varepsilon}^y \\ 0 & 0 & \mathrm{i}\frac{\lambda'}{2}\hat{\varepsilon}^x - \frac{\lambda'}{2}\hat{\varepsilon}^y & -\mathrm{i}\frac{\lambda'}{2}\hat{\varepsilon}^z \\ \hline \mathrm{i}\frac{\lambda'}{2}\hat{\varepsilon}^z & \mathrm{i}\frac{\lambda'}{2}\hat{\varepsilon}^x + \frac{\lambda'}{2}\hat{\varepsilon}^y & 0 & 0 \\ \mathrm{i}\frac{\lambda'}{2}\hat{\varepsilon}^x - \frac{\lambda'}{2}\hat{\varepsilon}^y & -\mathrm{i}\frac{\lambda'}{2}\hat{\varepsilon}^z & 0 & 0 \end{array}\right). \tag{18}$$

The total Hamiltonian matrix is the sum of matrices (17) and (18),

$$\hat{H} = \left(\begin{array}{cc|cc} \hat{\varepsilon}_{\mathbf{k}} + \mathrm{i}\frac{\lambda}{2}\hat{\varepsilon}^z & \mathrm{i}\frac{\lambda}{2}\hat{\varepsilon}^x + \frac{\lambda}{2}\hat{\varepsilon}^y & \mathrm{i}\frac{\lambda'}{2}\hat{\varepsilon}^z & \mathrm{i}\frac{\lambda'}{2}\hat{\varepsilon}^x + \frac{\lambda'}{2}\hat{\varepsilon}^y \\ \mathrm{i}\frac{\lambda}{2}\hat{\varepsilon}^x - \frac{\lambda}{2}\hat{\varepsilon}^y & \hat{\varepsilon}_{\mathbf{k}} - \mathrm{i}\frac{\lambda}{2}\hat{\varepsilon}^z & \mathrm{i}\frac{\lambda'}{2}\hat{\varepsilon}^x - \frac{\lambda'}{2}\hat{\varepsilon}^y & -\mathrm{i}\frac{\lambda'}{2}\hat{\varepsilon}^z \\ \hline \mathrm{i}\frac{\lambda'}{2}\hat{\varepsilon}^z & \mathrm{i}\frac{\lambda'}{2}\hat{\varepsilon}^x + \frac{\lambda'}{2}\hat{\varepsilon}^y & \hat{\varepsilon}_{\mathbf{k}+\mathbf{Q}} + \mathrm{i}\frac{\lambda}{2}\hat{\varepsilon}^z & \mathrm{i}\frac{\lambda}{2}\hat{\varepsilon}^x + \frac{\lambda}{2}\hat{\varepsilon}^y \\ \mathrm{i}\frac{\lambda'}{2}\hat{\varepsilon}^x - \frac{\lambda'}{2}\hat{\varepsilon}^y & -\mathrm{i}\frac{\lambda'}{2}\hat{\varepsilon}^z & \mathrm{i}\frac{\lambda}{2}\hat{\varepsilon}^x - \frac{\lambda}{2}\hat{\varepsilon}^y & \hat{\varepsilon}_{\mathbf{k}+\mathbf{Q}} - \mathrm{i}\frac{\lambda}{2}\hat{\varepsilon}^z \end{array}\right). \tag{19}$$

Number of electrons on a filled d-orbital of a single iron is 6 and we assume 2 orbitals to be completely filled, so for doping concentration x we have for the number of electrons on two irons $n = 2(6-2-x) = 2(4-x)$. Hereafter, the chemical potential μ is calculated to fulfill this criterion with $x = 0$.

3. Results for the Fermi surface and the band structure

Without the SO coupling ($\lambda = 0$) both the band structure and the Fermi surface are shown in Fig. 1. Topologically, the FS is different from that of Ref. [24] by the additional central FS sheet. Qualitatively, the FS is similar to those found in DFT calculations and five-orbital models [7,8].

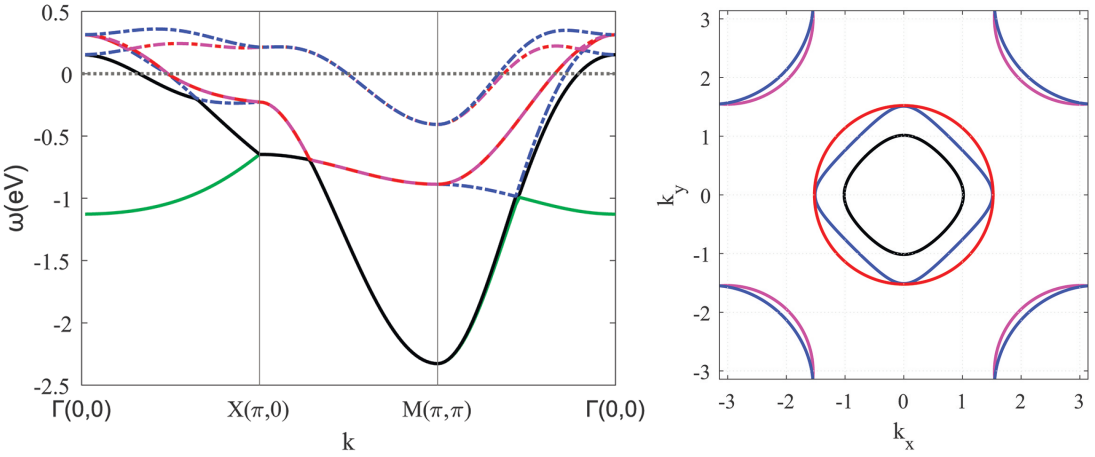

Fig. 1. Band structure and the Fermi surface in the three-orbital model without the SO coupling ($\lambda = \lambda' = 0$) in the 2-Fe BZ; $\mu = -0.0529$ eV. Bands are plotted relative to the chemical potential, so zero corresponds to μ

Effect of the intra-ion SO coupling is shown in Fig. 2, where $\lambda = 100$ meV and $\lambda' = 0$. The degeneracy of some bands is lifted at the Γ-point and the volume of the central FS sheet slightly changes. There is no topological difference to the FS results for the vanishing SO interaction.

If we switch on only the inter-ion SO interaction by setting $\lambda = 0$ and $\lambda' = 100$ meV, we end up with the splitting of the previously degenerate bands along the $X - M$ direction, see Fig. 3. It results in the topological change of the corresponding FS sheets around the M and symmetrical points — instead of the coinciding FS sheets along the $X - M$ direction, we have two separate ones.

Finite intra-ion and inter-ion SO couplings ($\lambda = \lambda' = 100$ meV) results in the band structure and FS shown in Fig. 4. Both the lifting of the degeneracy of some bands at the Γ-point and the splitting of the previously degenerate bands along the $X - M$ direction are present.

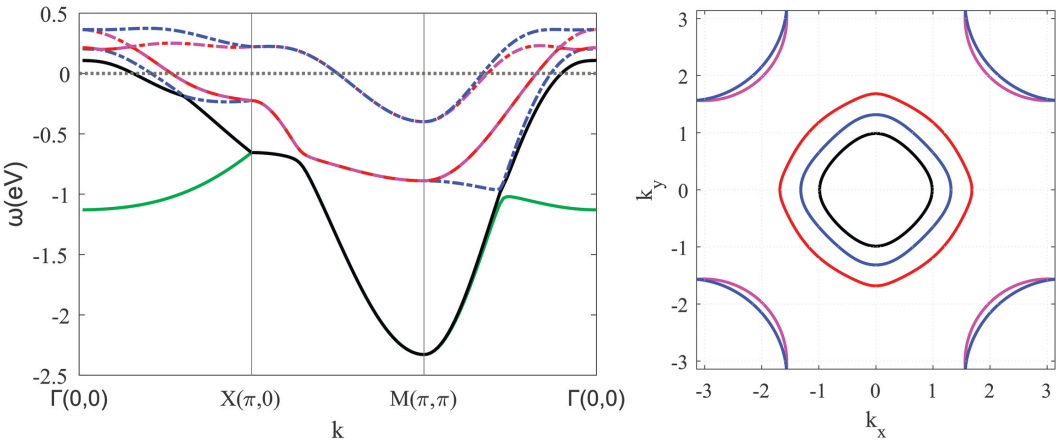

Fig. 2. The same as in Fig. 1 but for the finite intra-ion SO coupling $\lambda = 100$ meV and zero inter-ion SO coupling $\lambda' = 0$; $\mu = -0.0542\ eV$

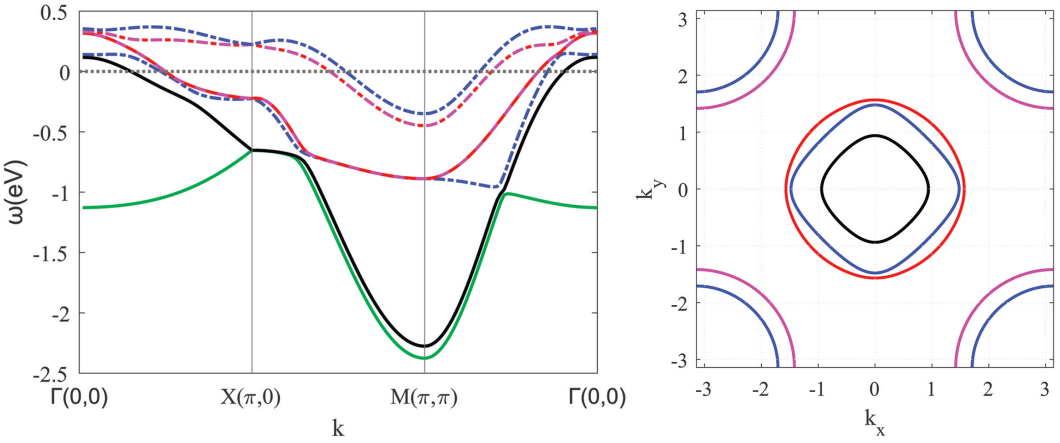

Fig. 3. The same as in Fig. 1 but for the finite inter-ion SO coupling $\lambda' = 100$ meV and zero intra-ion SO coupling $\lambda = 0$; $\mu = -0.0556\ eV$

FS topologically different from the FS without the SO coupling, similar to the case of finite inter-ion SO interaction.

Conclusions

Here we modified the interorbital hopping term of the three-orbital model to avoid the unphysical violation of the C_4 symmetry. Introducing the intra- and inter-ion SO coupling constants λ and λ' allows us to separate the effect of the related couplings on the band structure and the Fermi surface. We show that the SO interaction results in the topological changes of the Fermi surface. In particular, the inter-ion part of the SO coupling leads to the splitting of two FS sheets around the M-point. Without SO, they may be represented as two ellipses rotated by the $\pi/2$ relative to each other. With the finite SO coupling, they resemble two concentric circles with the center at the M-point. Apart from that, the lifting of the degeneracy of some bands at the Γ-point and the splitting of the previously degenerate bands along the $X - M$ direction appear due to the SO interaction.

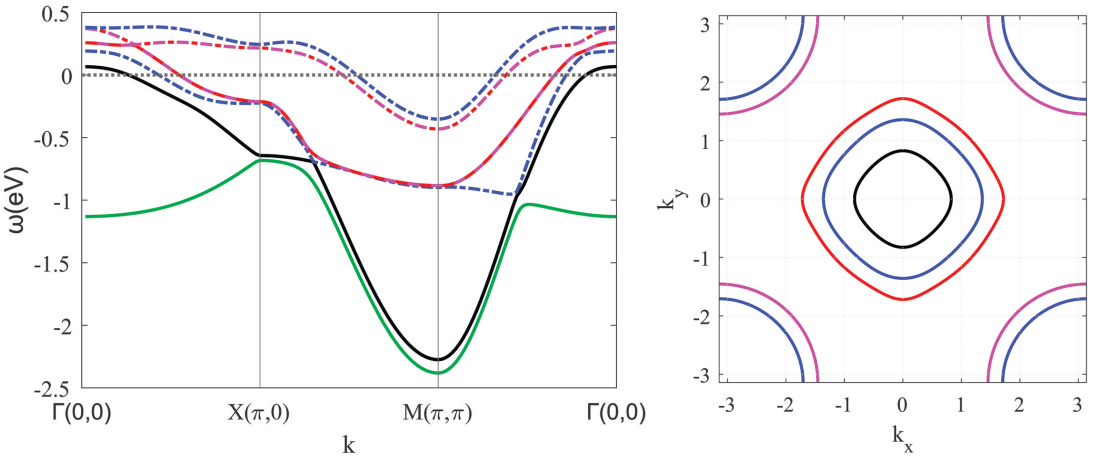

Fig. 4. The same as in Fig. 1 but for the finite intra- and inter-ion SO couplings, $\lambda = \lambda' = = 100$ meV; $\mu = -0.0567\ eV$

In the normal state, the change of the FS topology near the M-point should lead to the change of the dynamical spin response that is maximal at or near the wave vector connecting Γ and M-points. In the superconducting state, the obtained topology of the FS near the M-point may result in inequality between gaps on the inner and the outer FS sheets. Together with the gaps at the FS sheets near the Γ-point, it can give an explanation for the observation of the three different gaps in LiFeAs [17]. Another important consequence of the SO coupling is the possible realization of the nontrivial superconducting state. Since the spin becomes bad quantum number and the states are classified by the pseudospin, the superconducting order parameter may be composed of the spin-singlet and spin-triplet states [28].

Note that the study of LiFeAs material within the ten-orbital model [26] with the SO coupling results in qualitatively the same change of the FS topology and the band structure [27] if here we assume both finite λ and λ'. Folding procedure is absent in the ten-orbital model and the inter-ion SO interaction doesn't appear there in a direct form. Although the folding for the energies of the three-orbital model is a transparent procedure, for the wave functions it is a separate complicated task. Therefore, the introduction of the inter-ion SO interaction here in the form of Eq. (8) may be treated as an ansatz to simulate the results of the proper ten-orbital treatment that lacks the artificial folding procedure.

References

[1] P.J.Hirschfeld, Comptes Rendus Physique, **17**(2016), 197–231. DOI: 10.1016/j.crhy.2016.06.001

[2] J.Wang, Y.Wu, X.Zhou, Y.Li, B.Teng, P.Dong, J.He, Y.Zhang, Y.Ding, J.Li, *Advances in Physics: X*, **6**(2021), 1878931. DOI: 10.1080/23746149.2021.1878931

[3] R.M.Fernandes, A.I.Coldea, H.Ding, I.R.Fisher, P.J.Hirschfeld, G.Kotliar, *Nature*, **601**(2022), 35. DOI: 10.1038/s41586-021-04073-2

[4] P.J.Hirschfeld, M.M.Korshunov, I.I.Mazin, Gap symmetry and structure of Fe-based superconductors, *Rep. Prog. Phys.*, **74**(2011), 124508. DOI: 10.1088/0034-4885/74/12/124508

[5] M.M.Korshunov, I.Eremin, Doping evolution of itinerant magnetic fluctuations in Fe-based pnictides, *Europhys. Lett.*, **83**(2008), 67003. DOI: 10.1209/0295-5075/83/67003

[6] I.I.Mazin, D.J.Singh, M.D.Johannes, M.-H.Du, Unconventional Superconductivity with a Sign Reversal in the Order Parameter of $LaFeAsO_{1-x}F_x$, *Phys. Rev. Lett.*, **101**(2008), 057003. DOI: 10.1103/PhysRevLett.101.057003

[7] S.Graser, T.A.Maier, P.J.Hirschfeld, D.J.Scalapino, Near-degeneracy of several pairing channels in multiorbital models for the Fe pnictides, *New. J. Phys.* **11**(2009), 025016. DOI: 10.1088/1367-2630/11/2/025016

[8] K.Kuroki, S.Onari, R.Arita, H.Usui, Y.Tanaka, H.Kontani, H.Aoki, Unconventional Pairing Originating from the Disconnected Fermi Surfaces of Superconducting $LaFeAsO_{1-x}F_x$, *Phys. Rev. Lett.*, **101**(2008), 087004. DOI: 10.1103/PhysRevLett.101.087004

[9] S.Maiti, M.M.Korshunov, T.A.Maier, P.J.Hirschfeld, A.V.Chubukov, Evolution of the Superconducting State of Fe-Based Compounds with Doping, *Phys. Rev. Lett.*, **107**(2011), 147002. DOI: 10.1103/PhysRevLett.107.147002

[10] M.M.Korshunov, Superconducting state in iron-based materials and spin-fluctuation pairing theory, *Physics-Uspekhi*, **57**(2014), 813. DOI: 10.3367/UFNe.0184.201408h.0882

[11] O.J.Lipscombe, L.W.Harriger, P.G.Freeman, M.Enderle, C.Zhang, M.Wang, T.Egami, J.Hu, T.Xiang, M.R.Norman, P.Dai, Anisotropic neutron spin resonance in superconducting $BaFe_{1.9}Ni_{0.1}As_2$, *Phys. Rev. B*, **82**(2010), 064515. DOI: 10.1103/PhysRevB.82.064515

[12] M.M.Korshunov, Y.N.Togushova, I.Eremin, P.J.Hirschfeld, Spin-orbit coupling in Fe-based superconductors, *J. Supercond. Nov. Magn.*, **26**(2013), 2873. DOI: 10.1007/s10948-013-2212-6

[13] I.Eremin, D.Manske, K.H.Bennemann, Electronic theory for the normal-state spin dynamics in Sr_2RuO_4: Anisotropy due to spin-orbit coupling, *Phys. Rev. B*, **65**(2002), 220502(R). DOI: 10.1103/PhysRevB.65.220502

[14] D.Daghero, M.Tortello, G.A.Ummarino, R.S Gonnelli, *Rep. Prog. Phys.*, **74**(2011), 124509. DOI: 10.1088/0034-4885/74/12/124509

[15] T.E.Kuzmicheva, A.V.Muratov, S.A.Kuzmichev, A.V.Sadakov, Yu.A.Aleshenko, V.A.Vlasenko, V.P.Martovitsky, K.S.Pervakov, Yu.F.Eltsev, V.M.Pudalov, *Uspekhi Fizicheskikh Nauk*, **187**(2017), 450. DOI: 10.3367/UFNr.2016.10.038002

[16] T.E.Kuzmicheva, S.A.Kuzmichev, I.V.Morozov, S.Wurmehl, B.Büchner, *JETP Lett.*, **111**(2020), 350. DOI: 10.1134/S002136402006003X

[17] T.E.Kuzmicheva, S.A.Kuzmichev, *JETP Lett.*, **114**(2021), 630. DOI: 10.31857/S1234567823080098

[18] S.Raghu, X.-L.Qi, C.-X.Liu, D.J.Scalapino, S.-C.Zhang, Minimal two-band model of the superconducting iron oxypnictides, *Phys. Rev. B*, **77**(2008), 220503. DOI: 10.1103/PhysRevB.77.220503

[19] P.A.Lee, X.-G Wen, *Phys. Rev. B*, **78**(2008), 144517. DOI: 10.1103/PhysRevB.78.144517

[20] R.Yu, K.T.Trinh, A.Moreo, M.Daghofer, J.A.Riera, S.Haas, E.Dagotto, *Phys. Rev. B*, **79**(2009), 104510. DOI: 10.1103/PhysRevB.79.104510

[21] P.M.R.Brydon, C.Timm, *Phys. Rev. B*, **79**(2009), 180504. DOI: 10.1103/PhysRevB.81.014511

[22] M.Daghofer, A.Nicholson, A.Moreo, E.Dagotto, *Phys. Rev. B* , **81**(2010), 014511. DOI: 10.1103/PhysRevB.81.014511

[23] M.M.Korshunov, Y.N.Togushova, I.Eremin, *J. Supercond. Nov. Magn.*, **26**(2013), 2665. DOI: 10.1007/s10948-013-2156-x

[24] M.M.Korshunov, Y.N.Togushova, *J. Siberian Fed. Univ. Math. and Phys.*, **11**(2018), 430. DOI: 10.17516/1997-1397-2018-11-4-430-437.

[25] K.K.Ng, M.Sigrist, *Europhys. Lett.*, **49**(2000), 473. DOI: 10.1209/epl/i2000-00173-x

[26] Y.Wang, A.Kreisel, V.B Zabolotnyy, S.V.Borisenko, B.B uchner, T.A.Maier, P.J.Hirschfeld, D.J.Scalapino, *Phys. Rev. B*, **88**(2013), 174516. DOI: 10.1103/PhysRevB.88.174516

[27] M.M.Korshunov, Chapter "Itinerant Spin Fluctuations in Iron-Based Superconductors" in the book "Perturbation Theory: Advances in Research and Applications", ed. by Z. Pirogov, Nova Science Publishers Inc. New York, 2018, 61.

[28] V.P.Mineev, K.V.Samokhin, "Vvedenie v teoriyu neobychnoi sverhprovodimosti", Izdatelstvo MFTI Moscow, 1998; Translated as "Introduction to unconventional superconductivity", Gordon and Breach Scie. Publ. Amsterdam, 1999.

Изменение топологии поверхности Ферми в трехорбитальной модели пниктидов железа со спин-орбитальным взаимодействием

Данил А.Иванов
Юлия Н.Тогушова
Сибирский федеральный университет
Красноярск, Российская Федерация
Максим М.Коршунов
Институт физики им. Л. В. Киренского СО РАН
Красноярск, Российская Федерация
Сибирский федеральный университет
Красноярск, Российская Федерация

Аннотация. Изучено влияние спин-орбитального взаимодействия на зонную структуру и поверхность Ферми в трехорбитальной модели. Межорбитальная часть модели изменена для полного соответствия с симметрией решетки железа. Из-за наличия двух ионов железа в элементарной ячейке мы вводим внутри- и межионную константы спин-орбитального взаимодействия для разделения эффектов соответствующих взаимодействий на зонную структуру и поверхность Ферми. И внутри, и межионная части снимают вырождение некоторых зон в точке $\Gamma = (0, 0)$ и вырождение вдоль направления $(0, \pi) - (\pi, \pi)$ зоны Бриллюэна. Показано, что межионная часть спин-орбитального взаимодействия приводит к изменению топологии поверхности Ферми, а именно к разделению листов поверхности Ферми вблизи точки $M = (\pi, \pi)$.

Ключевые слова: сверхпроводники на основе железа, спин-орбитальное взаимодействие, зонная структура, поверхность Ферми.